Acta Chemica Scandinavica, 1994: 48: 290–293
Printed in Belgium – all rights reserved

ACTA
CHEMICA SCANDINAVICA
ISSN 0904–213X

Properties of Ni_3S_2 at High Temperatures

Helmer Fjellvåg[a,*] and Arnfinn Andersen[b]

[a]Department of Chemistry, University of Oslo, N-0315 Oslo, Norway and [b]SINTEF SI, N-0314 Oslo, Norway

Fjellvåg, H. and Andersen, A., 1994. Properties of Ni_3S_2 at High Temperatures. – Acta Chem. Scand. 48: 290–293 © Acta Chemica Scandinavica 1994.

The structural properties of the two modifications of Ni_3S_2 are reported. In α-Ni_3S_2 at low temperature the Ni atoms occupy tetrahedral sites, and any homogeneity range is very limited up to the transformation into β-Ni_3S_2 at 838 ± 5 K. Unit-cell data are provided for the extremely defect, ionic-conducting β-Ni_3S_2 phase as a function of composition and temperature. Thermal expansion data are presented for both modifications. The structure of β-Ni_3S_2 is considered in relation to other fast-ionic conductors with a face-centered cubic sublattice of anions.

Nickel and nickel alloys may undergo severe corrosion at temperatures between 800 and 1100 K in sulfur-containing atmospheres.[1,2] Normally, the reaction is passivated by a protective oxide film. However, rapid corrosion occurs when Ni_3S_2 is formed as a reaction product in the NiO matrix of the corrosion layer. This feature has been interpreted in terms of nickel diffusion being several orders of magnitude larger in Ni_3S_2 than in NiO.[3]

Studies of corrosion reactions[2] have shown that Ni_3S_2 forms an interconnected network along NiO grain boundaries of the corrosion scale, and thereby increases the reaction rates significantly, although present as a minority phase. Thus the properties of Ni_3S_2 have great technological relevance. However, more knowledge of its high-temperature properties, with respect to crystal and defect structure and diffusion properties, is desirable for understanding the corrosion reactions.

The Ni–S binary system contains a number of phases. Several of these are fairly well characterized,[4] whereas for others, e.g. Ni_7S_6, the situation is still unclear.[5] Among the Ni–S phases, Ni_3S_2 constitutes the most nickel-rich solid phase. Ni_3S_2 exists in two modifications, α-Ni_3S_2 at low temperatures $T \leq 838$ K, and β-Ni_3S_2 at higher temperatures. The rhombohedral α-phase transforms discontinuously into the cubic β-phase. Whereas α-Ni_3S_2 shows no homogeneity range at room temperature, β-Ni_3S_2 extends over a wide composition interval. The crystal structure of α-Ni_3S_2 (heazlewoodite) has been questioned; however, single-crystal X-ray diffraction studies have confirmed the structure originally described by Westgren.[6–8] Recently, single crystals of Ni_3S_2 were re-examined by Metcalf *et al.*[9] Thermodynamic data for Ni–S phases have recently been published by Stølen *et al.*[10]

The object of the present contribution is to report on structural properties and on variations in composition at elevated temperatures for α- and β-Ni_3S_2. Since β-Ni_3S_2 is not quenchable, all studies on the phase were made within its range of thermal stability. Thermal expansion data for the two polymorphs of Ni_3S_2 are given, and features of the crystal structure of β-Ni_3S_2 are discussed.

Experimental

Samples of Ni_tS_2 ($2.6 \leq t \leq 3.4$) were prepared by heating weighed amounts of the pure elements (Ni, turnings from rods, 99.99%, Johnson, Matthey & Co. and S, lumps, 99.999%, Koch-Light Laboratories) in evacuated, sealed silica glass tubes. After a first heat treatment at 600 °C for 1 d followed by crushing at room temperature, re-annealing was carried out at 600 °C for 3 d before the samples were slowly cooled to room temperature during 1 d. Samples with $t > 3.0$ then contain Ni as a minority phase, whereas those with $t < 3.0$ contain additional β-Ni_9S_8 or one of the metastable forms of Ni_7S_6.[5]

All samples were studied by room- and high-temperature powder X-ray diffraction (PXD), respectively, in a Guinier camera ($CuK\alpha_1$ radiation, Si as internal standard) and in a Guinier–Simon camera ($CuK\alpha_1$ or $MoK\alpha_1$ radiation, 300 to 1300 K, temperature increase synchronized with film movement, heating rate 25–50 K h^{-1}). Powder neutron diffraction (PND) data were collected with the OPUS III two-axis diffractometer at the JEEP II reactor, Kjeller, at a wavelength of 187.7 pm. Diffraction data were collected for $5 \leq 2\Theta \leq 100°$ in steps of 0.05°. Refinements for α-Ni_3S_2 were carried out using the Hewat version[11] of the Rietveld program.[12] The scattering lengths $b_{Ni} = 10.3$ and $b_S = 2.85$ fm were taken from Ref. 13. Structure considerations for β-Ni_3S_2 were based

* To whom correspondence should be addressed.

on structure factors derived from integrated intensities deduced from powder X-ray diffraction photographs taken at 900 K. A Nicolet LS18 microdensitometer and the SCANPI[14] and GX[15] program systems were used.

Results and discussion

(i) The low-temperature α-Ni_3S_2 phase. At 300 K, the rhombohedral unit cell has dimensions $a = 407.9 \pm 0.1$ pm and $\alpha = 89.47 \pm 0.01°$ (cf. Ref. 9 and references therein). No systematic extinctions were indicated by the PXD and PND data, and the refinements confirmed the space group to be *R*32. The Ni and S atoms occupy 3(*e*) and 2(*c*) positions, respectively, (1/2, *y*, *y*) and (*x*, *x*, *x*). The unconstrained positional parameters are $y_{Ni} = 0.2457 \pm 0.0003$ and $x_S = 0.2546 \pm 0.0012$ (22 reflections; $R_N = 0.040$; $a = 407.89 \pm 0.01$ pm, $\alpha = 89.45 \pm 0.01°$). The parameters agree well with data published by Fleet[7] and by Parise,[8] in contrast to the recent data provided by Metcalf *et al.*[9]

The sulfur atoms in rhombohedral α-Ni_3S_2 build a nearly body-centered cubic arrangement, of which a subset of tetrahedral holes are occupied by nickel atoms. The four Ni–S bonding distances are split into two sets, with distances 226.4 ± 0.5 (2 ×) and 227.9 ± 0.5 (2 ×) pm. The nickel atoms are furthermore coordinated by four other Ni-atoms at 250.4 ± 0.2 (2 ×) and 252.8 ± 0.2 (2 ×) pm. The short Ni–Ni distances comply with those of metallic Ni, and among the Ni–S phases such short distances are only found for β-Ni_9S_8.[16]

The variations of the unit-cell dimensions between 300 and 800 K are shown in Fig. 1. Whereas *a* increases, α decreases with increasing temperature (in the trigonal setting of the unit cell, both axes increase). The thermal expansion is non-linear (Fig. 1). On average, the linear volume thermal expansion coefficient is $\alpha_V = (1/V)(\Delta V/\Delta T) = 4.7 \times 10^{-5}\ K^{-1}$.

The refined unit-cell parameters for α-Ni_3S_2 in samples with different nominal composition *t* were compared. At 295 K no variations in the unit-cell parameters larger than two calculated standard deviations were found. At 800 K, non-systematic variations in *V* of up to four calculated standard deviations occured, probably as a result of the less accurate Guinier–Simon technique (with no internal standard). This clearly indicates that any homogeneity range of α-Ni_3S_2 must be very small compared with that of β-Ni_3S_2 (see below). If a volume increment of 10^7 pm^3 per Ni atom is assumed, the variation at

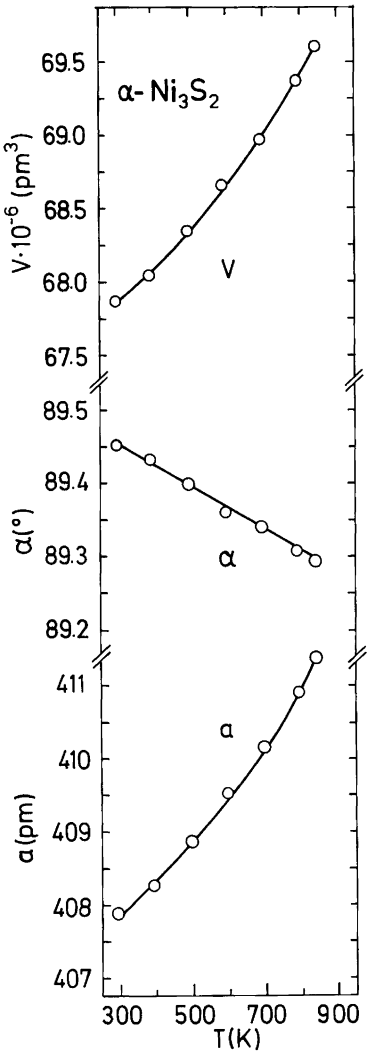

Fig. 1. Temperature dependence of unit-cell dimensions for α-Ni_3S_2.

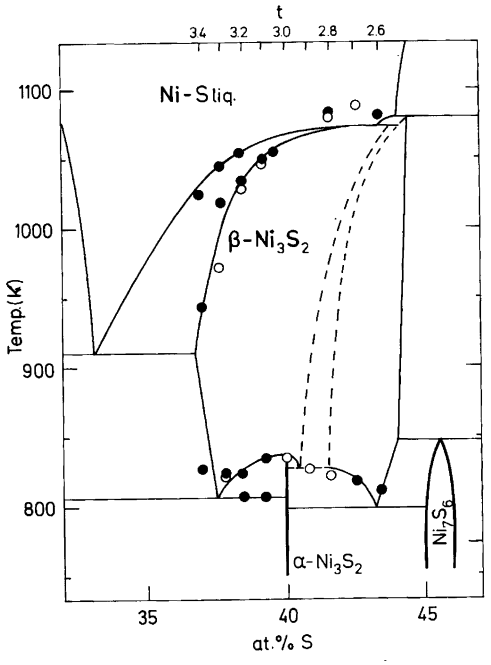

Fig. 2. Section of the Ni–S phase diagram. Solid line, according to Kullerud and Yund,[4] dotted line, two-phase region proposed by Lin *et al.*;[17] filled and open circles present results from DTA and PXD, respectively.

800 K, if it exists, corresponds to a maximum variation in the Ni content of ± 0.014 atoms per unit cell.

(ii) The high-temperature β-Ni_3S_2 phase. α-Ni_3S_2 transforms at $T_d = 838 \pm 5$ K into cubic β-Ni_3S_2 according to DTA and PXD data. The temperature-dependent homogeneity region for β-Ni_3S_2 is shown in Fig. 2 (evaluated from DTA and PXD data) and agrees well with the findings by Kullerud and Yund[14] and by Lin *et al.*[17]

The high-temperature PXD experiments were hampered by NiO formation at some 900 K, but this problem was overcome by using double, evacuated and sealed quartz capillaries. The small, and highly symmetric, unit cell for β-Ni_3S_2 required Mo$K\alpha_1$ radiation in order for intensity data to be collected for the largest possible number of reflections. Cu$K\alpha_1$ radiation was used for collection of thermal expansion data. No single crystal of β-Ni_3S_2 could be obtained, probably owing to the destructive β-to-α phase transition on cooling.

The variation of the unit-cell dimensions a and V with composition t at 920 K is shown in Fig. 3. A smooth, almost linear relation between a and t is found. Any partial oxidation of the samples was easily recognized from the observed temperature variation of the unit-cell dimensions, since oxidation shifts the composition of the β-Ni_3S_2 phase towards the sulfur-rich phase boundary; e.g. for $Ni_{3.2}S_2$ the a-axis was found to shorten continuously and approached that for $t = 2.8$ at 1050 K (in addition NiO was observed).

The temperature variations of the a-axis for $t = 2.8$, 3.1 and 3.3 are shown in Fig. 4. The average volume thermal expansion coefficient does not vary significantly with t, and α_V equals 6×10^{-5} K^{-1}, which is somewhat larger than for α-Ni_3S_2. Lin *et al.*[17] modified the original phase diagram forwarded by Kullerud and Yund,[4] and suggested that two different phases, separated by a small two-phase region, actually exist within the wide domain of solid solubility (cf. dotted lines in Fig. 2). From the numerous high-temperature diffraction experiments no confirmation of a two-phase region was possible.

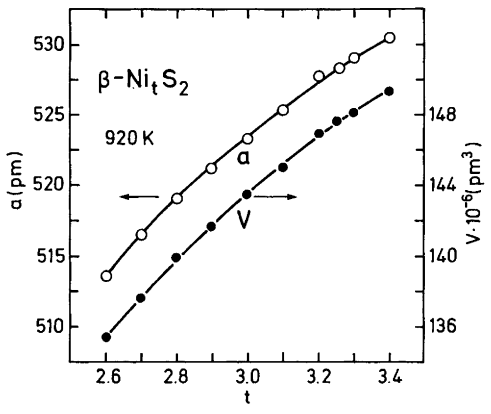

Fig. 3. Variation of a-axis and unit-cell volume for β-Ni_3S_2 at 920 K.

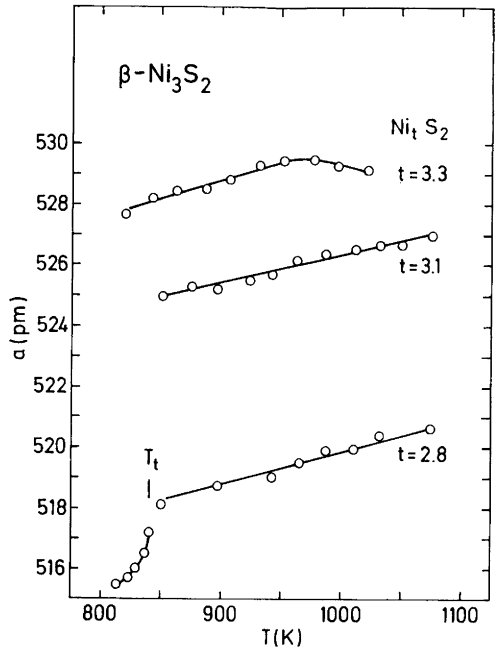

Fig. 4. Temperature dependence of a-axis between 800 and 1080 K for the β-Ni_3S_2 phase for the compositions $Ni_{2.8}S_2$, $Ni_{3.1}S_2$ and $Ni_{3.3}S_2$.

The temperature dependences of the unit-cell dimensions shown in Fig. 4 contain additional details related to the phase diagram (Fig. 2). The onset of the deviation of $a(T)$ for $Ni_{3.3}S_2$ from linearity correlates in temperature with the onset of partial melting. For the nominal composition $Ni_{2.8}S_2$, the α- and β-Ni_3S_2 phases coexist in a narrow temperature interval. By using data in Fig. 3 and $\alpha_V = 6 \times 10^{-5}$ K^{-1}, a composition $t = 2.65$ is calculated for the β-Ni_3S_2 phase at 810 K, in good agreement with phase-diagram data. Over the temperature range 810–840 K the continuous change in composition of the β-Ni_3S_2 phase (cf. phase diagram, Fig. 2) results in a large increase of the a-axis.

All strong reflections in the PXD diagrams for β-Ni_3S_2 are accounted for by an F-type Bravais lattice. In a few of some 25 high-temperature runs, definite evidence for other reflections, such as (110) and (332), was present. No indications for deviations from cubic symmetry were found. The sparse PXD data showed no reflections for d-values less than 100 pm, probably owing to huge displacement factors for the disordered phase. Only 8 reflections were observed for $Ni_{2.6}S_2$ with $I > 3\sigma(I)$ (using Mo$K\alpha_1$ radiation; 900 K). In addition, 8 reflections were considered to have zero observed intensity. A proper analysis of the structure on this basis became impossible. Nevertheless, different models and various space groups were tested. The structure is most probably closely related to a defect antifluorite-type structure, with face-centering of sulfur atoms. However, owing to some of the observations regarding Bragg reflections (see above), the distribution of the Ni atoms cannot be face-centered

cubic for the entire composition/temperature stability range of the phase. Attempts to refine the disordered structure on the basis of high-temperature PND and PXD (collected with synchrotron radiation) data did not give unambiguous results. Actually, the disorder on the metal sublattice is so large that the Bragg reflection intensities, even in the case of the strongly scattering Ni atoms in the PND diagrams, are very low compared with the background and fall off rapidly with increasing scattering angle.[18] New PND experiments at high temperatures using position-sensitive detectors will be carried out.

For $Ni_{2.6}S_2$, with $Z = 2$, the 5.2 nickel atoms of the unit cell may occupy tetrahedral sites (at a distance of 225 pm to sulfur), octahedral sites with a Ni–S distance of 260 pm, or distorted sites with Ni–S distances between 205 and 275 pm. Preliminary refinements (for PXD intensity data, see above) indicate distribution of the Ni atoms (*viz.* split atoms) over positions situated close to the tetrahedral sites, but shifted towards the side of the 'ideal' tetrahedron. It should be noted that higher-order terms for the temperature factor description should in principle be adopted for the case with mobile cations, which, however, would require access to single-crystal diffraction data.

The enthalpy and entropy changes for the α-to-β transformation are substantial,[10] and exceed those of the fast-ionic conductors Ag_2S,[19] Cu_2S[20] and AgI.[21] In particular, the enthalpy change at the α-to-β transition is larger than that for the melting of β-Ni_3S_2.[10] Furthermore, data on Ni self-diffusion are available for α-Ni_3S_2[22] as well as for the chemical diffusion coefficient in β-Ni_3S_2.[23] However, the conductivity has a significant electronic component, and metallic behaviour is reported.[9,17,23] Whereas some fast-ionic conducting chalcogenides have a basically body-centered arrangement of anions (β-Ag_2S in an intermediate temperature range,[24] α-Ag_2Se,[25] α-AgI at high temperatures[26] and Ag_3SI[27]), a face-centered arrangement of anions is found for Cu_2S,[28] Cu_2Se,[28] Li_2S[29] and Na_2S.[30] A common feature for the latter phases is a shift of the cations out of the tetrahedral sites (in split model calculations; harmonic temperature factor description) and a small, yet significant, occupancy of deformed octahedral sites. For the space group *Fm3m* this corresponds to shifts from the 8(*c*) position (1/4, 1/4, 1/4) into (*x*, *x*, *x*) or (*x*, *x*, *z*) positions, and a partial filling of (1/2, 0, 0) or (*x*, 0, 0). More reliable structure data for β-Ni_3S_2 are required for a proper comparison with the situation among the group of defect anti-fluorite-type ionic conductors.

References

1. Andersen, A., Haflan, B., Kofstad, P. and Lillerud, K. P. *Mater. Sci. Eng. 87* (1987) 45.
2. Alcock, C. B., Hocking, M. G. and Zador, S. *Corros. Sci. 9* (1969) 111.
3. Luthra, K. L. and Worell, W. L. *Metall. Trans. 9A* (1978) 1055.
4. Kullerud, G. and Yund, R. A. *J. Petrol. 3* (1962) 126.
5. Seim, H., Stølen, S., Fjellvåg, H., Grønvold, F. and Westrum, E. F., Jr. *To be published.*
6. Westgren, A., *Z. Anorg. Chem. 239* (1938) 82.
7. Fleet, M. E. *Am. Mineral. 62* (1977) 341.
8. Parise, J. *Acta Crystallogr. Sect. B36* (1980) 1179.
9. Metcalf, P. A., Fanwick, P., Kakol, Z. and Honig, J. M. *J. Solid State Chem. 104* (1993) 81.
10. Stølen, S., Grønvold, F., Westrum, E. F., Jr. and Kolonin, G. R. *J. Chem. Thermodyn. 23* (1991) 77.
11. Hewat, A. W. *UKAERE Harwell Report RRL 73/897*, Harwell 1973.
12. Rietveld, H. K. *J. Appl. Crystallogr. 2* (1969) 65.
13. Koester, L. and Yelon, W. B. In: Yelon, W. B., Ed., *Neutron Diffraction Newsletter*, The Neutron Diffraction Commission, Missouri 1983.
14. Werner, P. E. *The Computer Program SCANPI*, Institute of Inorganic Chemistry, University of Stockholm, Stockholm, Sweden 1981.
15. Mallinson, P. R. and Muir, K. W. *J. Appl. Crystallogr. 18* (1985) 51.
16. Fleet, M. E. *Can. Miner. 26* (1988) 283.
17. Lin, R. Y., Hu, D. C. and Chang, Y. A. *Metall. Trans. B9* (1978) 531.
18. Fjellvåg, H. *Unpublished results.*
19. Grønvold, F. and Westrum, E. F., Jr. *J. Chem. Thermodyn. 18* (1986) 381.
20. Grønvold, F. and Westrum, E. F., Jr. *J. Chem. Thermodyn. 19* (1987) 1183.
21. Shaviv, R., Westrum, E. F., Jr., Grønvold, F., Stølen, S., Inaba, A., Fujii, H. and Chihara, H. *J. Chem. Thermodyn. 21* (1989) 631.
22. Bestow, B. D. and Wood, G. C. *Oxid. Met. 9* (1975) 473.
23. Yagi, H. and Wagner, J. B. *Oxid. Met. 18* (1982) 41.
24. Cava, R. J., Reidinger, F. and Wuensch, B. J. *J. Solid State Chem. 31* (1980) 69.
25. Oliveira, M., McMullan, R. K. and Wuensch, B. J. *Solid State Ionics 28–30* (1988) 1332.
26. Cava, R. J., Reidinger, F. and Wuensch, B. J. *Solid State Commun. 24* (1977) 411.
27. Didisheim, J.-J., McMullan, R. K. and Wuensch, B. J. *Solid State Ionics 18–19* (1986) 1150.
28. Yamamoto, K. and Kashida, S. *J. Solid State Chem. 93* (1991) 202.
29. Altorfer, F., Bührer, W., Anderson, I., Schärpf, O., Bill, H., Carron, P. L. and Smith, H. G. *Solid State Ionics Proc. Symp. A2* (1991) 325.
30. Altorfer, F., Bührer, W., Carron, P. L. and Bill, H. *Progress Report ETH Zürich and Paul Scherrer Institut, LNS-167*, 1993, p. 154.

Received August 5, 1993.